Solid-State Structure of Copolyesters Containing a Mesogenic Monomer

Y. S. Hu, R. Y. F. Liu, D. A. Schiraldi, A. Hiltner,* and E. Baer

Department of Macromolecular Science and Center for Applied Polymer Research, Case Western Reserve University, Cleveland, Ohio 44106-7202

Received August 22, 2003

ABSTRACT: This study examined the solid-state structure of copolyesters based on smectic poly(diethylene glycol 4,4′-bibenzoate) (PDEGBB) and non-liquid crystalline poly(diethylene glycol isophthalate) (PDEGI). The isophthalate content was varied from 10 to 50 mol %. Differential scanning calorimetry (DSC), Fourier transform infrared (FTIR) spectroscopy, wide-angle X-ray diffraction (WAXD), dynamic mechanical thermal analysis (DMTA), and tapping mode atomic force microscopy (AFM) were employed to characterize the polymers. The combined observations suggest that the PDEGBB-I copolymers fall into two classes depending upon isophthalate content. Copolymers with up to 20% isophthalate content possess some amount of liquid crystalline (LC) character. They exhibit a smectic-to-isotropic transition in DSC, smectic layer reflections in WAXD, and lamellar structures in AFM. It appears that isophthalate groups are excluded from the smectic layers and therefore are very effective in disrupting long-range LC order. Copolymers with 30% or more isophthalate are amorphous. These materials do not exhibit crystalline or LC character after exposure to the thermal histories used in this study. The Fox equation describes the dependence of glass transition temperature (T_g) from loss modulus on copolymer composition for non-LC glasses and predicts that the T_g of glassy PDEGBB is 14 °C higher than the observed T_g of the LC glass.

Introduction

Thermotropic liquid crystalline polymers (LCPs) have been of interest as engineering plastics because of their low viscosity and ease of orientation, their high strength, and their high barrier performance. However, they are expensive and often require high process temperatures. Furthermore, phase transitions occur rapidly, which can make control of solid-state structure difficult. Copolymerization is widely used to extend the structure−property spectrum of polymers in general.[1] Efforts to copolymerize a mesogenic monomer with a nonmesogenic monomer have focused primarily on reducing the melting temperature in order to facilitate processing.[2−5] For example, copolymerization with 50 mol % *p*-phenylene isophthalate units reduces the melting point of intractable poly(*p*-oxybenzoate) from >460 to 345 °C and into the processable range.[3]

Copolymerization with a nonmesogenic monomer also has the effect of disrupting the LC texture as observed in the light microscope. Depending on the chemical structure of the monomers, the amount of a nonmesogenic unit that can be tolerated before the LC order is completely destroyed varies from 30 to 70 mol %.[6−8] Not surprisingly, nonlinear monomers are more effective in destroying LC order than linear monomers. Incorporation of 30% of a nonlinear bisphenol or nonlinear dicarboxylic acid completely destroys the liquid crystallinity of a nematic aromatic polyester.[6] However, poly(hexamethlyene-4,4′-bibenzoate-*co*-2,6-naphthalate) retains smectic order with up to 60 mol % naphthalate.[8]

It can be anticipated that copolymerization with a nonmesogenic monomer will compromise the outstanding barrier properties of LCPs to some extent. However, this aspect has not been examined. Candidate copolymers for such a study are copolyesters based on 4,4′-bibenzoate as the mesogenic unit. Polyesters of 4,4′-bibenzoic acid and aliphatic diols longer than two carbon atoms are thermotropic LCPs with relatively low transition temperatures.[9−11] The solid-state structure and oxygen barrier properties of smectic poly(diethylene glycol 4,4′-bibenzoate) (PDEGBB) were the subject of a recent study.[12] A hierarchical structural model for smectic PDEGBB was proposed on the basis of the combined results of atomic force microscopy (AFM) and wide-angle X-ray diffraction (WAXD) in which mesogens organized into smectic layers, stacks of layers formed wavy lamellae, and assemblies of lamellae defined domains. The hierarchical structure provided the basis for understanding the excellent oxygen barrier of PDEGBB and revealed a liquid crystalline state intermediate between the permeable amorphous glass and the impermeable 3-dimensional crystal.

It is appropriate to extend the previous study to copolymers based on PDEGBB that incorporate a nonmesogenic monomer. Isophthalate is chosen for this purpose because its nonlinear structure is expected to efficiently disrupt the LC order of PDEGBB.[3,4] The solid-state structure of PDEGBB, poly(diethylene glycol isophthalate) (PDEGI), and their copolymers is described in this paper. A structural model is extracted from the combined results of thermal behavior, conformational analysis, WAXD, dynamic mechanical response, and morphology by AFM. The oxygen barrier properties of this family of polymers will be discussed in a companion paper.[13]

Materials and Methods

Poly(diethylene glycol 4,4′-bibenzoate) (PDEGBB), poly(diethylene glycol isophthalate) (PDEGI), and their copolymers with 10, 20, 30, 40, and 50 mol % isophthalate were provided by KoSa (Spartanburg, SC) in the form of extruded pellets. The chemical structure of PDEGBB-I copolymers is shown in Chart 1. The copolymers are identified as PDEGBB-*x*I, where *x* is the mole percent isophthalate.

Polymers were prepared by melt polymerization. The homopolymer PDEGBB was prepared by combining 337.5 g (1.25 mol; KoSa) of 4,4′-bibenzoic acid dimethyl ester with 298.4 g of diethylene glycol (2.81 mol; 2.25:1 mole ratio; Aldrich) and 0.15 g of tetrabutyl titanate catalyst ([Ti] = 65 ppm; Aldrich) in a 2 L 316-stainless steel three-neck polymerization reactor

* Corresponding author: e-mail pah6@cwru.edu.

10.1021/ma030439m CCC: $27.50
Published on Web 02/25/2004

Table 1. Composition and Intrinsic Viscosity of PDEGBB-I Copolymers

designation	PDEGBB	PDEGBB-10I	PDEGBB-20I	PDEGBB-30I	PDEGBB-40I	PDEGBB-50I	PDEGI
mol % isophthalate	0	10	20	30	40	50	100
wt % isophthalate	0	7.8	16	25	34	43	100
intrinsic viscosity (dL g^{-1})	0.61	0.62	0.65	0.66	0.68	0.69	1.12

Chart 1

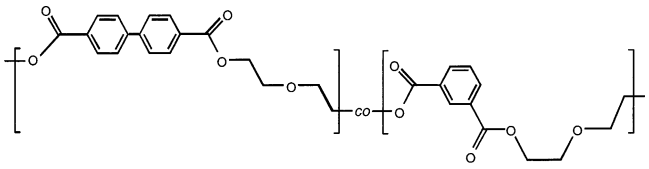

equipped with a mechanical agitator, methanol distillation column, gas adaptor, and an electric heating mantle. The reaction mixture was purged with nitrogen and heated to 240 °C over 90 min with 82 mL of methanol collected. After methanol evolution concluded, the distillation head was replaced with a vacuum adaptor, the reactor temperature was increased to 250 °C, and vacuum was applied over 30 min. After an additional 220 min polymerization time, the resultant polymer was extruded through an opening at the bottom of the reactor and quenched in ambient temperature water.

In the same manner, the PDEGBB-*x*I polymers were produced by replacing *x* mol % of 4,4′-bibenzoic acid dimethyl ester with *x* mol % of dimethyl isophthalate (Aldrich). All other reagents and conditions were equivalent to those of the homopolymer. Randomization of copolymers was virtually ensured under the melt-polymerization process that was utilized.[14] Because the polyesters were living condensation polymers, polydispersities of approximately 2.0 were always obtained under conditions of melt polymerization. The viscosity was measured at 25 °C in 1% (w/w) dichloroacetic acid solution. The intrinsic viscosity was calculated using the parameters for PET homopolymer and therefore should be considered a "pseudo-intrinsic viscosity". Composition and intrinsic viscosity of the copolymers are listed in Table 1. The comonomer content is given as the reaction feed.

After the pellets were dried in vacuo for 24 h at a temperature between ambient and 80 °C depending on the comonomer content, they were compression-molded between Teflon-coated aluminum sheets in a press at 250 °C (40 °C above the clearing point of PDEGBB) to obtain films 180−200 μm thick. The platens were heated in the press for 3 min with repeated application and release of pressure to remove air bubbles and held at 309 psi (2.1 MPa) for an additional 3 min. Quenched films were taken rapidly from the isotropic melt into iced water. It was not possible to quench PDEGBB and PDEGBB-10I to the amorphous state due to the extremely rapid isotropic to liquid crystalline transition. Copolymers with more than 30% isophthalate were quenched into the amorphous state. Quenched films were used for characterization unless otherwise indicated. Other films were slowly cooled in the press at approximately 2 °C min^{-1} from 250 °C through the isotropic to liquid crystalline transition to a predetermined temperature and quenched into ice water; i.e., PDEGBB was slowly cooled to 155 °C, PDEGBB-10I to 120 °C, PDEGBB-20I to 80 °C, and PDEGBB-30I to 40 °C.

Thermal analysis was conducted with a Perkin-Elmer DSC-7 calibrated with indium and tin. Heating and cooling scans were performed under nitrogen at 10 °C min^{-1} over the temperature range from 0 to 280 °C.

Dynamic mechanical measurements were carried out in a dynamic mechanical thermal analyzer (DMTA) Mk II unit from Polymer Laboratories (Amherst, MA) operating in the tensile mode, using a frequency of 1 Hz and heating rate of 3 °C min^{-1}.

Wide-angle X-ray diffraction (WAXD) powder patterns were obtained at ambient temperature with a Philips diffractometer in the transmission mode using a slit angle of 1/12°. The oriented X-ray patterns were recorded using a Statton camera and Ni-filtered Cu Kα radiation calibrated with calcium fluoride. Quenched films were oriented by cold drawing to a draw ratio of 5.0 at a rate of 30% min^{-1} at a temperature approximately 20 °C above T_g. The drawn films were subsequently heat-set under tension at a temperature below the LC to isotropic transition.

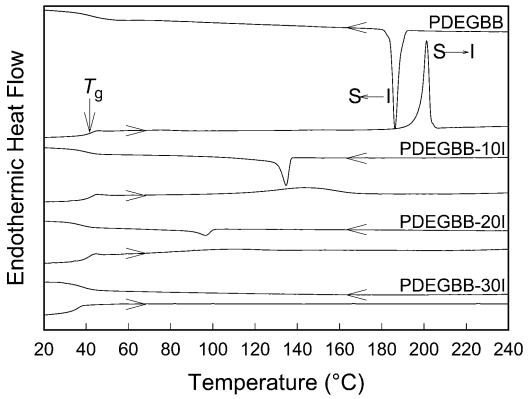

Figure 1. Thermograms of PDEGBB, PDEGBB-10I, PDEGBB-20I, and PDEGBB-30I cooled from the isotropic melt to the glassy state at 10 °C min^{-1} and reheated at 10 °C min^{-1}.

Conformational composition was determined by photoacoustic Fourier transform infrared (FTIR) spectroscopy. Spectra were collected at ambient temperature with a Nicolet 870 FTIR spectrometer using a MTEC model 200 photoacoustic cell. Specimens were cut from the molded films and dried overnight in vacuo at ambient temperature to remove moisture. For each specimen, 256 scans were collected with a resolution of 4 cm^{-1} and mirror velocity of 0.158 cm s^{-1}. All spectra were internally normalized using the carbonyl stretching band at about 1730 cm^{-1}, which has been demonstrated to be stable during orientation and crystallization of PET.[15,16]

Free surfaces were prepared for atomic force microscopy (AFM). Small pieces of the pellet were sandwiched between clean glass cover slides, heated into the isotropic state (about 230 °C) on the hot stage of an optical microscope, and lightly pressed to spread out the melted polymer. After the specimen was removed from the hot stage and cooled to ambient temperature, one of the cover slides was peeled off to create a free surface. The specimen with the free surface was vacuum-dried, remelted under nitrogen, and subjected to a thermal history that mimicked the compression-molded films, i.e., quenched or slowly cooled. The free surfaces were etched with 40 wt % aqueous methylamine solution at 23 °C using the procedures of Organ et al.[17] The etched specimens were washed with deionized water and methanol. The optimum etching time was 48 h for PDEGBB, 6 h for PDEGBB-10I, and 0.5 h for PDEGBB-20I and PDEGBB-30I. Initially the specimens were about 35−50 μm in thickness. Etching removed material from the surface to a depth of about 150−400 nm. Images of the etched surfaces were obtained in air at ambient conditions using the Nanoscope IIIa MultiMode head from Digital Instruments (Santa Barbara, CA). Experiments were conducted in the tapping mode using Si probes with 50 N m^{-1} spring constant and resonance frequencies in the range 284−362 kHz. The tip had a radius of 10 nm. Height and phase images were recorded simultaneously.

Results and Discussion

Thermal Behavior. The thermograms of PDEGBB, PDEGBB-10I, PDEGBB-20I, and PDEGBB-30I in Figure 1 were obtained by cooling from 280 to 0 °C at a rate of 10 °C min^{-1}, followed by heating at the same rate. The cooling curve of the homopolymer contained

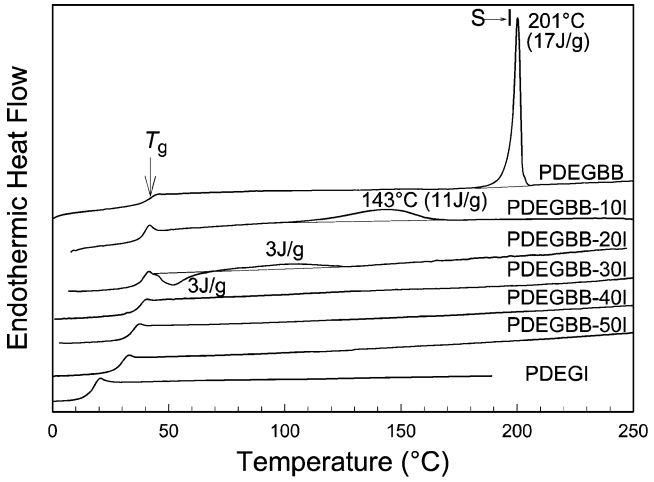

Figure 2. Heating thermograms of quenched PDEGBB-I copolymers.

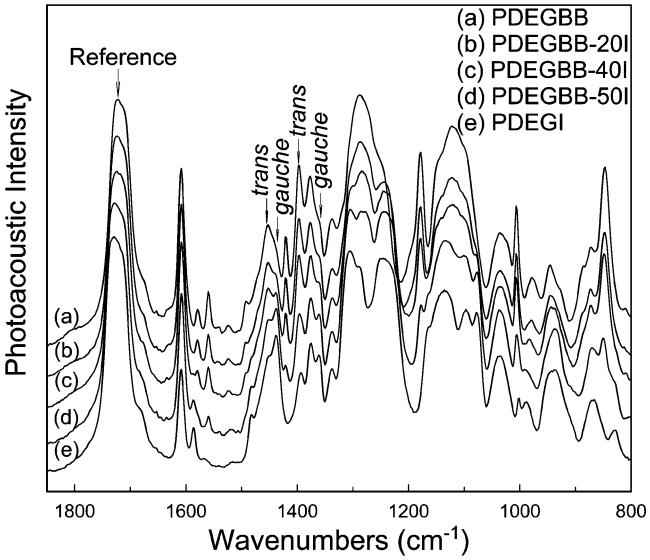

Figure 3. Representative FTIR spectra of quenched PDEGBB-I copolymers.

Table 2. Properties of Quenched PDEGBB-I Copolymers

	DSC				
samples	T_g (°C)	ΔC_p (J g^{-1} °C^{-1})	DMTA (tan δ) T_g (°C)	DMTA (E'') T_g (°C)	trans fraction f_t
PDEGBB	42	0.26	52	45	0.79
PDEGBB-10I	39	0.26	49	45	0.76
PDEGBB-20I	36	0.26	47	44	0.72
PDEGBB-30I	34	0.31	46	41	0.71
PDEGBB-40I	32	0.35	44	38	0.70
PDEGBB-50I	28	0.36	42	34	0.65
PDEGI	16	0.42	28	22	0.46

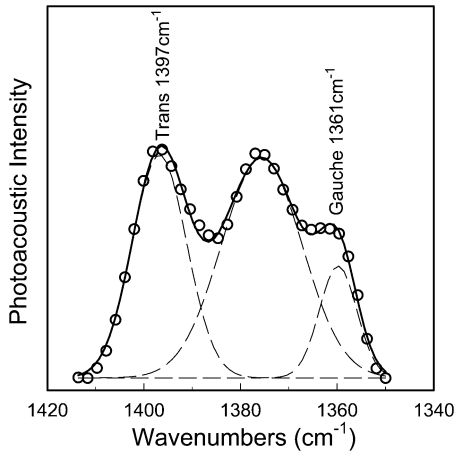

Figure 4. Deconvolution of the 1410−1350 cm^{-1} region of the infrared spectrum to obtain peak heights of trans and gauche bands for quenched PDEGBB-50I.

a sharp peak at 186 °C with an exothermic heat of 17 J g^{-1} followed by the glass transition at 42 °C. The heating curve showed a sharp endothermic peak at 201 °C. The small supercooling identified the transition as liquid crystalline. A previous study showed it to be the smectic CA to isotropic (S−I) transition.[12] The absence of crystallization and melting peaks categorized PDEGBB as an LC glass. With increasing isophthalate content, the liquid crystalline transition broadened, shifted to a lower temperature, and decreased in enthalpy. Cooling thermograms of PDEGBB-10I and PDEGBB-20I had the I−S transition at 135 and 96 °C with heats of 11 and 3 J g^{-1}, respectively. Subsequent heating curves revealed a very broad S−I transition centered at 143 and 108 °C, respectively. These trends reflected the progressive decrease in length and concentration of liquid crystalline DEGBB sequences. Cooling and heating thermograms of PDEGBB-30I showed only the glass transition at 35 °C.

The thermograms in Figure 2 were obtained by heating compression-molded films that had been quenched from the isotropic melt. Quenched PDEGBB and PDEGBB-10I exhibited the glass transition and S−I transition as in Figure 1. Quenched PDEGBB-20I exhibited the glass transition followed by an exothermic peak at 53 °C, which was due to formation of liquid crystalline order from the isotropic rubber. A broad S−I transition appeared at a higher temperature. Apparently the DEGI sequences retarded the I−S transition enough that PDEGBB-20I could be quenched almost to the isotropic glass. Upon heating above T_g, the copolymer underwent cold liquid crystallization similar to cold crystallization of many quenched non-LC polyesters.[18] For copolymers with higher isophthalate content and for PDEGI, only the glass transition was observed. With T_g of 16 °C, PDEGI was in the rubbery state at ambient temperature. The T_g and heat capacity jump ΔC_p at T_g of all the quenched films are listed in Table 2.

Conformational Analysis. The ethylene vibrational regions in the infrared spectra of PDEGBB-I copolymers (Figure 3) closely resembled those of non-LC aromatic polyesters. Band assignments were made accordingly. Specific bands assigned to trans and gauche conformers appeared in three regions of the spectrum: 1500−1400 cm^{-1} (region I), 1400−1300 cm^{-1} (region II), and 1000−800 cm^{-1} (region III). Characteristic conformational peaks associated with ethylene linkages of PDEGBB-I copolymers were assigned as follows: 1452 cm^{-1} (trans) and 1438 cm^{-1} (gauche) in region I and 1397 cm^{-1} (trans),[19] 1361 cm^{-1} (gauche),[20] and 1338 cm^{-1} (trans) in region II. In region III, the trans and gauche bands were less distinct. The trans band near 970 cm^{-1} appeared to split into three peaks and shifted with isophthalate content. The gauche band near 898 cm^{-1} was obscured by neighboring peaks. Conformational analysis utilized bands in regions I and II.

The 1410−1350 cm^{-1} region was deconvoluted into three Gaussian peaks as illustrated in Figure 4. The trans (1397 cm^{-1}) and gauche (1361 cm^{-1}) peak heights were normalized to the carbonyl stretching band near

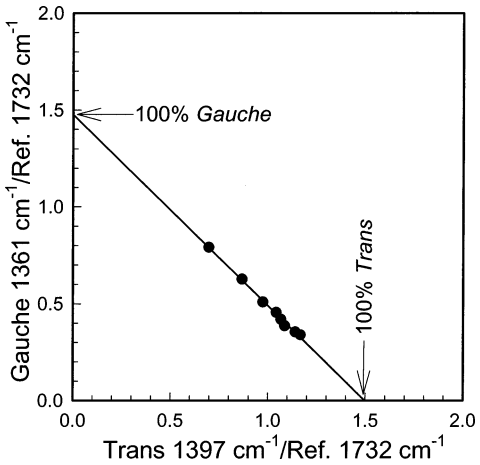

Figure 5. Normalized peak heights of the gauche and trans infrared bands of quenched PDEGBB-I copolymers.

1730 cm^{-1}. The relative amount of trans and gauche conformers was determined by plotting the normalized peak heights as in Figure 5. Excellent linearity was obtained. Extrapolation gave intercepts that corresponded to the normalized band intensities for 100% trans and 100% gauche conformers. It can be seen from the intercepts that the trans and gauche bands used in the analysis had about the same molar absorptivity.

The trans fraction, defined as $f_t = A/A_0$ where A is the normalized 1397 cm^{-1} peak height and A_0 is the normalized 1397 cm^{-1} peak height for 100% trans conformers, is tabulated in Table 2 for quenched copolymers. The PDEGBB trans fraction of 0.79 closely correlated with results from conformational calculations (80%),[21] and molecular simulation (82%),[22] for other LCPs. The high trans fraction was consistent with the relatively extended conformation of an LCP. Disruption of chain linearity by incorporation of isophthalate groups gradually decreased the trans fraction to 0.65 for PDEGBB-50I and 0.46 for PDEGI. A trans fraction of 0.46 appeared rather high for a glassy, non-LC aromatic polyester. Aromatic polyesters with ethylene glycol spacers usually have lower trans fraction, typically less than 0.2 in the isotropic glass.[16,23] The longer DEG spacer might have favored a higher fraction of trans conformations. Furthermore, isophthalate tends to increase the trans fraction; e.g., poly(ethylene isophthalate) has a trans fraction of 0.25 compared to 0.10 for amorphous PET.[24]

A pair of conformational bands in the 1500−1410 cm^{-1} region, 1452 cm^{-1} (trans) and 1438 cm^{-1} (gauche), were analyzed in the same fashion. This region was used previously to obtain conformer compositions of aromatic polyesters.[16] The trans fraction determined from this region was systematically 4−6% lower than that determined from the 1410−1350 cm^{-1} region. The difference was probably due to extensive overlap in the 1500−1410 cm^{-1} region, which gave rise to mixed conformational modes. Nevertheless, the trends were the same.

Wide-Angle X-ray Diffraction (WAXD). The WAXD pattern of quenched PDEGBB film exhibited a sharp peak at $2\theta = 5.65°$ (15.6 Å) (Figure 6), corresponding to the spacing of the smectic layers.[12] This spacing was less than the calculated length of the fully extended repeat unit of 18.2 Å. It was frequently observed with smectic LCPs that the layer spacing measured from WAXD was less than the fully extended length. The difference was attributed to the presence of some gauche

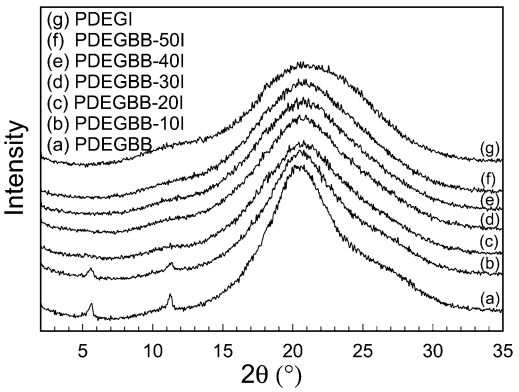

Figure 6. WAXD scans of quenched PDEGBB-I copolymer films.

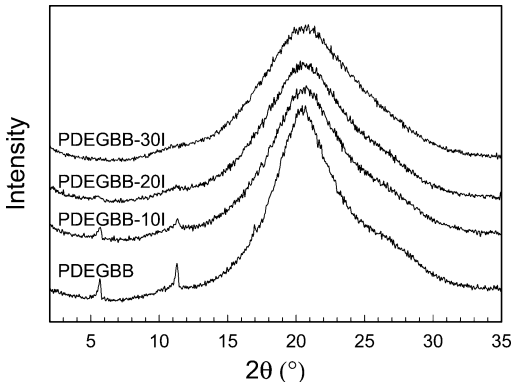

Figure 7. WAXD scans of slowly cooled PDEGBB-I copolymer films.

or eclipsed conformations of the spacer.[25,26] The trans fraction of 0.79 determined from infrared analysis allowed for a significant fraction of non-trans conformations in smectic PDEGBB. The second-order reflection of the layer spacing at 11.3° was also clearly distinguishable. A broad reflection centered at 20.5° was attributed to disordered lateral packing of the mesogens.

In PDEGBB-10I, the layer reflection at 5.65° was broader and less intense, and the amorphous reflection centered at 20.5° was broader than in PDEGBB; however, there was no change the layer spacing (Figure 6). Other quenched copolymers and PDEGI showed only broad reflections with no evidence of smectic character, in agreement with DSC results. The amorphous reflection at about 20.5° gradually broadened as the isophthalate content increased from quenched PDEGBB-20I to PDEGI. It was speculated that quenched PDEGBB-20I possessed some lateral order without the longitudinal registry that defines a mesophase.[27] Broadening of the reflection as the isophthalate content increased suggested that the lateral order was gradually lost. The parallel decrease in trans fraction (Table 2) was consistent with this interpretation.

Slow cooling of PDEGBB and PDEGBB-10I intensified the layer reflection at 5.65° and the second-order reflection at 11.3° (Figure 7). The third-order reflection at 17.0° was discernible in slow-cooled PDEGBB. No change of the layer spacing was observed. It appeared that slow cooling produced an LC glass with the same smectic CA structure as quenching, but with slightly better order. Slow-cooled PDEGBB-20I developed a very broad layer reflection in the WAXD pattern. However PDEGBB-30I did not show LC order even after slow cooling. Nonlinear comonomers appeared to be particu-

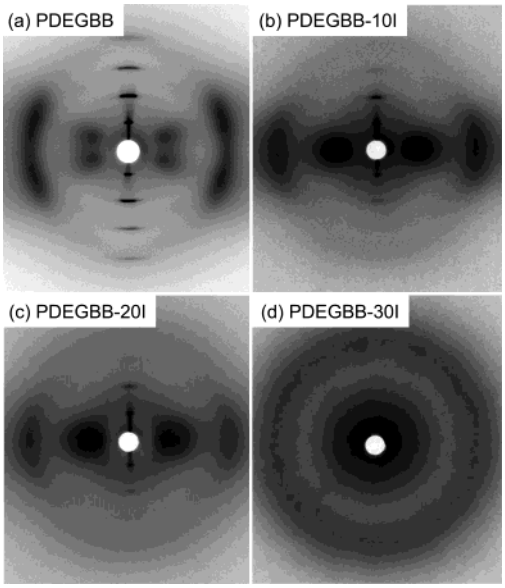

Figure 8. WAXD patterns of oriented films: (a) PDEGBB oriented at 65 °C and heat-set at 155 °C for 6 h under tension; (b) PDEGBB-10I oriented at 62 °C and heat-set at 90 °C for 3 h under tension; (c) PDEGBB-20I oriented at 55 °C and heat-set at 70 °C for 3 h under tension; and (d) PDEGBB-30I oriented at 50 °C and heat-set at 60 °C for 2 h under tension. Orientation direction is vertical.

larly effective in disrupting LC order. A similar amount of a nonlinear bisphenol or nonlinear dicarboxylic acid completely destroyed the liquid crystallinity of a nematic aromatic polyester.[6] In contrast, more than 60 mol % 2,6-naphthalate was required to completely disrupt the smectic order of poly(hexamethylene 4,4′-bibenzoate-*co*-2,6-naphthalate).[8]

The diffraction pattern of the stretched PDEGBB film revealed the orientation of the mesogens in the smectic layers (Figure 8a). The layer reflections formed arcs on the meridian with a spacing of 15.8 Å, essentially the same as in the quenched film. The pattern contained higher-order reflections up to the fourth order. The broad reflection at 20.5° was split into two arcs above and below the equator. These results indicated that the smectic layer normal was parallel to the orientation direction, and the mesogenic groups were tilted with respect to the orientation direction. The tilt angle measured directly from the splitting of the equatorial reflections was 20° to the layer normal, in good agreement with literature results.[28] Tilt of the mesogens differentiates the smectic CA form from the smectic A form, which has the mesogens oriented normal to the smectic plane.[29]

Stretched PDEGBB-10I and PDEGBB-20I films showed arcs on the meridian having the same spacing as PDEGBB but fewer higher-order reflections (Figure 8b,c). The third-order reflection was the highest detected in the PDEGBB-10I pattern, and only the second order was discernible in the PDEGBB-20I pattern. The broad equatorial arc was not split. On the basis of thermal analysis, PDEGBB-10I and PDEGBB-20I contained significantly less LC character than PDEGBB. Possibly, orientation of non-LC chains during drawing was "frozen in" by constraints imposed by the LC domains. Equatorial intensity from the oriented amorphous fraction could have hidden the split arcs of the LC phase. The PDEGBB-30I pattern did not show any chain orientation even with an apparent draw ratio of 5.0

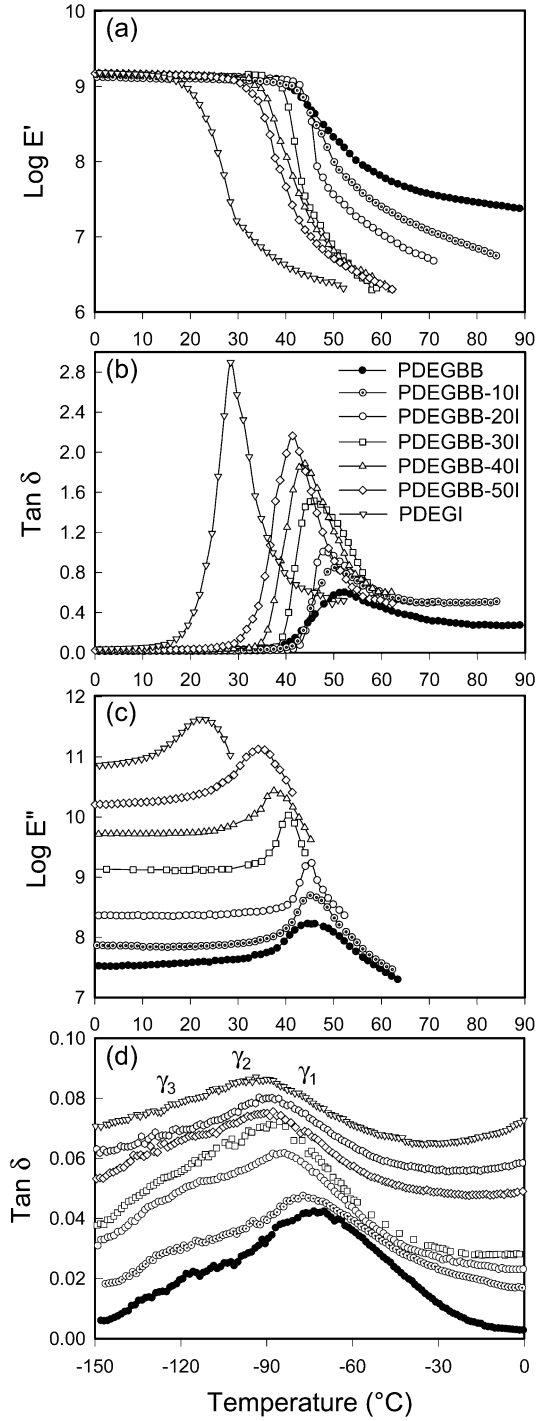

Figure 9. DMTA curves of quenched PDEGBB-I copolymers: (a) log E'; (b) tan δ; (c) log E'' with curves shifted vertically; and (d) low-temperature range of tan δ with curves shifted vertically.

(Figure 8d). Without the constraints imposed by LC domains, amorphous chains relaxed rapidly at the heat-set temperature 25 °C above the T_g.[14]

DMTA. Representative DMTA scans of quenched films in Figure 9 show storage modulus (E'), loss modulus (E''), and loss tangent (tan δ) as a function of temperature. The β-relaxation in Figure 9a−c corresponds to the glass transition.[30,31] The temperature of the tan δ peak is about 10 °C higher than the glass transition temperature in DSC scans (Table 2). The peak temperature of 52 °C for PDEGBB is in close agreement with literature reports.[30] Although the tan

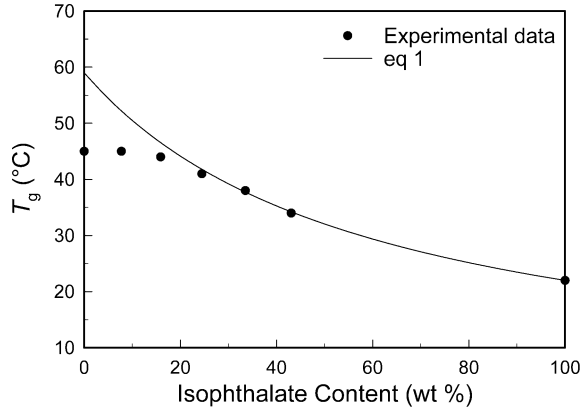

Figure 10. Glass transition temperature measured from log E'' as a function of weight percent isophthalate. The solid line describes the fit with the Fox law (eq 1).

δ peak of PDEGBB is recognized as the glass transition, the relaxation strength as indicated by peak intensity is much lower than is typical. The peak tan δ value of about 0.60 is only about one-quarter that of non-LC PDEGI. The accompanying drop in E' of 1.5 orders of magnitude is correspondingly less than the drop of 3 orders of magnitude observed with PDEGI. Somewhat surprisingly, copolymerization with 20% or 30% isophthalate caused the E'' peak of PDEGBB to become sharper; whereas increasing isophthalate content further again broadened the E'' peak.

The temperature of the E'' peak is plotted in Figure 10 as a function of isophthalate content. The T_g of amorphous, statistical copolymers usually follows the Fox law

$$\frac{1}{T_g} = \frac{w_1}{T_{g1}} + \frac{w_2}{T_{g2}} \quad (1)$$

where w_i refers to the weight fraction of component i in the copolymer and T_{gi} refers to the glass transition temperature of component i homopolymer. Achieving a satisfactory fit of eq 1 with T_g of non-LC PEGBB-I copolymers required the T_g of amorphous PDEGBB to be considerably higher than the observed T_g of smectic PDEGBB. The solid line in Figure 10 is the fit to eq 1 with T_g of amorphous PDEGBB equal to 59 °C, which is 14 °C higher than the observed T_g of the LC glass. It is frequently reported that the LC glass has a lower T_g than the amorphous glass.[8,32−35] It was found that a smectic poly(ether ester) derived from hydroxybibenzoic acid and (*R*,*S*)-2-methylpropane-1,3-diol had T_g 6 °C lower than its amorphous counterpart.[35] Also, the T_g of Vectra-like copolyesters and terpolyesters in the LC state was about 30 °C lower than that of the isotropic state.[33] The lower T_g of the LC glass was attributed to restricted segmental motion of chains in the LC domains.[33,35] Conformational analysis and X-ray diffraction indicate that highly extended conformers predominate in the LC phase. Segmental movement above the glass transition should not modify this orientation significantly, and therefore segmental movement should be more restricted than in the amorphous state. The free volume necessary to perform these rotations is considerably smaller than the free volume for segmental motion in the isotropic melt. Consequently, according to free volume theory, the glass transition of the liquid crystalline phase is reached at a lower temperature than the glass transition of the isotropic state. However, there

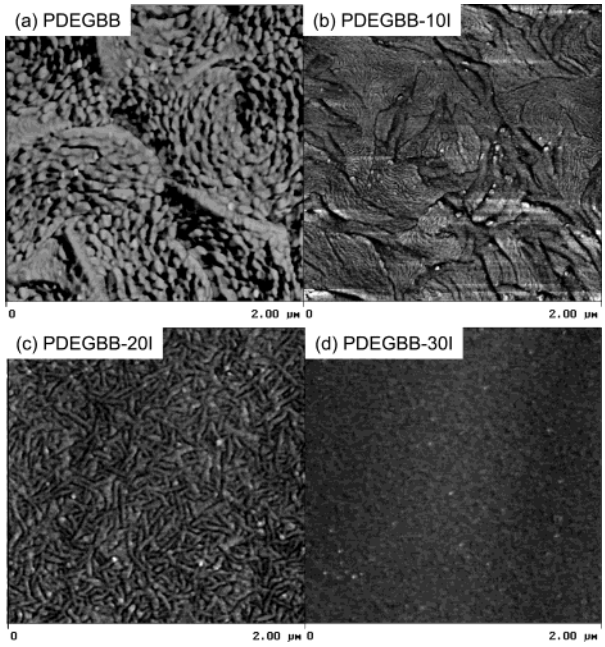

Figure 11. AFM phase images of slowly cooled PDEGBB-I copolymers: (a) PDEGBB after 48 h etch; (b) PDEGBB-10I after 6 h etch; (c) PDEGBB-20I after 0.5 h etch; and (d) PDEGBB-30I after 0.5 h etch.

are also reports that the LC glass has a higher T_g than the amorphous counterpart owing to decreased molecular mobility.[36−39]

The γ-relaxation at −70 to −120 °C is characteristic of aromatic polyesters with flexible spacers. It is generally thought that the broad peak encompasses several relaxation processes involving spacer and ester linkages.[40−44] The complexity of the γ-relaxation leads to identification of a higher temperature component (γ_1 at about −70 °C) with trans conformations of the spacer and a lower temperature component (γ_2 at about −100 °C) with gauche conformations of the spacer.[23,45] Increasing isophthalate content causes a significant shift of the γ-peak to lower temperature (Figure 9d), which is interpreted as a decrease in intensity of the γ_1-relaxation relative to the γ_2-relaxation. This is consistent with the increase in trans fraction from FTIR analysis. The total intensity of the γ-peak decreases from PDEGBB to PDEGI because the 1,3-attachment of ester groups limits the motions of phenyl ring and ester linkage.[46] A third component (γ_3 at about −120 °C) shows no remarkable dependence on comonomer content.

Morphology. The morphology of the LC glass was probed with specimens that were slowly cooled through the I−S transition. A 3 μm AFM image of the etched PDEGBB surface (Figure 11a) displayed polygonal domains in accordance with a previous study.[12] The domains were on the 2−3 μm size scale. The supermolecular texture within the domains consisted of arrays of short lamellae with thickness of 70 nm. Such lamellar structures have been reported frequently in smectic and nematic LCPs.[47−50]

Domains of slow-cooled PDEGBB-10I were slightly smaller, about 1 μm in size (Figure 11b). The AFM image revealed two types of lamellae. Arrays of very fine lamellae with thickness of 15 nm made up the domains. These lamellae were much thinner than those comprising the domains of PDEGBB. Superimposed on the domains of very fine lamellae was a network of single

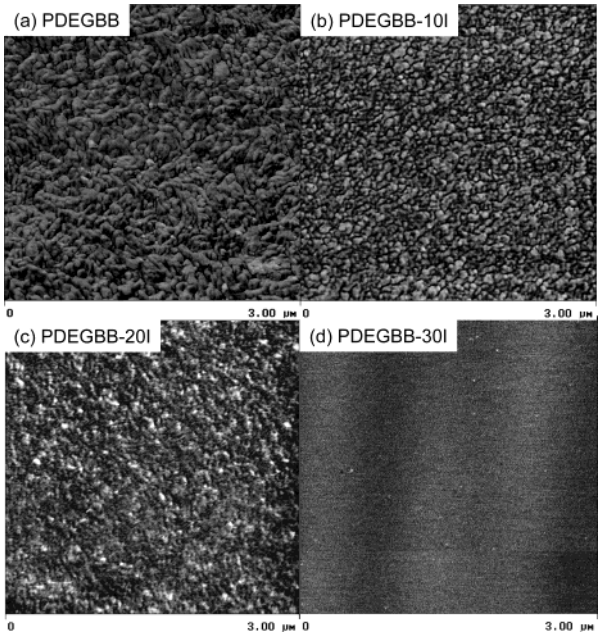

Figure 12. AFM phase images of quenched PDEGBB-I copolymers: (a) PDEGBB after 48 h etch; (b) PDEGBB-10I after 6 h etch; (c) PDEGBB-20I after 0.5 h etch; and (d) PDEGBB-30I after 0.5 h etch.

or small assemblies of much thick lamellae. These lamellae had about the same thickness, 70 nm, as those of PDEGBB.

Slow-cooled PDEGBB-20I did not exhibit domains. Only short curving lamellae about 35−40 nm thick were observed in the AFM image (Figure 11c). In thickness, the lamellae were intermediate between the thick and thin lamellae of PDEGBB-10I. The lamellae were randomly arrayed with only an occasional stack of two or more aligned lamellae. Slow-cooled PDEGBB-30I, which did not exhibit LC character in DSC thermograms or WAXD, was featureless in AFM images (Figure 11d).

Morphologies produced by quenching through the I−S transition were more poorly ordered than slow-cooled morphologies (Figure 12). Quenching prevented formation of large well-defined domains in PDEGBB (Figure 12a). Assemblies of a few aligned lamellae constituted poorly defined domains on the size scale of 150−500 nm. The short, densely packed lamellae of quenched PDEGBB were slightly thinner than those of slow-cooled PDEGBB, 50 nm compared to 70 nm. Domains could not be discerned in the AFM image of quenched PDEGBB-10I (Figure 12b). Instead, an overall granular texture dominated the morphology. The granules were about 50−100 nm in size. The AFM image of PDEGBB-20I showed possible evidence of a very fine granular texture (Figure 12c). The image of quenched PDEGBB-30I was virtually featureless (Figure 12d).

Model. The structural model presented for slow-cooled PDEGBB-I copolymers extends a previously proposed model for glassy PDEGBB[12] to incorporate the effect of a non-LC comonomer. As shown in Figure 13, more or less extended chains of PDEGBB assemble with the mesogenic bibenzoate groups organized into smectic layers. From WAXD, the smectic layers are oriented perpendicular to the chain axis and individual mesogens within the smectic layer are tilted at a slight angle to the chain direction.[12] The spacing of the smectic layers is 1.56 nm from WAXD, which is less than the extended chain dimension, estimated at 1.82 nm. This may be a

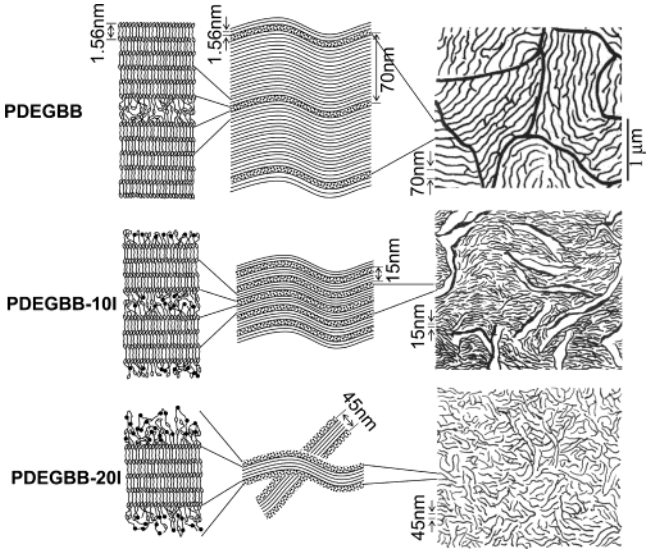

Figure 13. Hierarchical model of slowly cooled PDEGBB, PDEGBB-10I, and PDEGBB-20I.

general feature of smectic LCPs and indicates some gauche kinks or eclipsed conformations. Stacks of smectic layers form lamellae seen in the AFM images. The lamellar thickness of 70 nm corresponds to a stack with 45 smectic layers. Regular stacking of the smectic layers is periodically interrupted by disordered regions that contain chain ends, chain folds, and other chain defects. The periodic interruptions of the regular stacking define the thickness of the lamellae. Assemblies of lamellae constitute domains on the micron size scale. A domain in the liquid crystalline context is a region within which an orientation parameter varies no more than slowly with position compared with its rapid variation or discontinuity at the delineating boundaries.

Copolymerization with isophthalate effectively reduces the amount of LC character as indicated by thermal analysis. However, copolymerization does not affect the LC layer spacing in the WAXD pattern, which suggests that the isophthalate groups are excluded from the smectic layers. Thus, copolymerization reduces the LC content without altering its basic structure. If the amount of isophthalate is low, runs of DEGBB are long enough to form stacks of smectic layers. However, regular stacking of smectic layers is frequently interrupted by isophthalate groups, which are rejected along with other chain defects. It appears from AFM that isophthalate at the 10% level can be accommodated in the interlamellar regions without destroying the characteristic LC structure of uniform lamellae assembled into domains. However, frequent interruption of the smectic layer stacking leads to considerable reduction in lamellar thickness from 70 nm for PDEGBB to 15 nm for PDEGBB-10I, corresponding to a reduction in the number of stacked layers from 45 to 10. As the isophthalate content increases, more material is rejected from the smectic layers and interlamellar registry is lost. The copolymer with 20% isophthalate forms a disordered array of short lamellae. With 30% isophthalate, runs of DEGBB are not long enough or numerous enough to assemble as smectic layers, and the copolymers do not exhibit any LC character even when slowly cooled at 2 °C min^{-1}.

Conclusions

The isophthalate group is very effective in disrupting long-range LC order. Only PDEGBB-I copolymers with 20 mol % isophthalate or less are capable of forming some amount of LC order. Isophthalate decreases the amount of LC character and decreases the temperature of the smectic-to-isotropic transition. Formation of LC order is inhibited by isophthalate to the extent that the copolymer with 20% isophthalate can be quenched almost to the amorphous glass; LC order develops only upon heating the quenched glass above T_g or upon slowly cooling from the melt. The Fox equation describes the dependence of T_g (from loss modulus) on copolymer composition for non-LC glasses and predicts that the T_g of glassy PDEGBB is 14 °C higher than the observed T_g of the LC glass. The decrease in glass transition temperature from 41 °C for the copolymer with 30% isophthalate to 22 °C for PDEGI homopolymer encompasses ambient temperature.

It appears that isophthalate groups are excluded from the smectic layers. Copolymers with up to 20% isophthalate contain runs of DEGBB that are long enough to form stacks of smectic layers. However, regular stacking of smectic layers is frequently interrupted by isophthalate groups, which are rejected along with other chain defects. Isophthalate at the 10% level can be accommodated in the interlamellar regions without destroying the characteristic LC structure, which consists of uniform lamellae assembled into domains. However, frequent interruption of the smectic layer stacking leads to considerable reduction in lamellar thickness from 70 nm for PDEGBB to 15 nm for the copolymer with 10% isophthalate. This corresponds to a reduction in the number of stacked layers from 45 to 10. As more material is rejected from the smectic layers, interlamellar registry is lost. The copolymer with 20% isophthalate forms a disordered array of short lamellae. When the isophthalate content is more than 20%, runs of DEGBB are not long enough or numerous enough to assemble as smectic layers. Copolymers with more than 20% isophthalate form amorphous glasses. They do not exhibit crystalline or LC character after exposure to the thermal histories used in this study.

Acknowledgment. Financial support of KoSa is gratefully acknowledged.

References and Notes

(1) Bensason, S.; Minick, J.; Moet, A.; Chum, S.; Hiltner, A.; Baer, E. *J. Polym. Sci., Part B: Polym. Phys.* **1996**, *34*, 1301−1315.
(2) Jackson, W. J., Jr. *Br. Polym. J.* **1980**, *12*, 154−162.
(3) Erdemir, A. B.; Johnson, D. J.; Tomka, J. G. *Polymer* **1986**, *27*, 441−447.
(4) Rosenau-Eichin, R.; Ballauff, M.; Grebowicz, J.; Fischer, E. W. *Polymer* **1988**, *29*, 518−525.
(5) Cai, R.; Samulski, E. T. *Macromolecules* **1994**, *27*, 135−140.
(6) Lenz, R. W.; Jin, J.-I. *Macromolecules* **1981**, *14*, 1405−1411.
(7) Lenz, R. W. *Faraday Discuss. Chem. Soc.* **1985**, *79*, 21−32.
(8) Tokita, M.; Osada, K.; Watanabe, J. *Polym. J.* **1998**, *30*, 589−595.
(9) Krigbaum, W. R.; Asrar, J.; Toriumi, H.; Ciferri, A.; Preston, J. *J. Polym. Sci., Polym. Lett. Ed.* **1982**, *20*, 109−115.
(10) Meurisse, P.; Noel, C.; Monnerie, L.; Fayolle, B. *Br. Polym. J.* **1981**, *13*, 55−63.
(11) Jackson, W. J., Jr.; Morris, J. C. In *Liquid-Crystalline Polymers*; Weiss, R. A., Ober, C. K., Eds.; American Chemical Society: Washington, DC, 1990; Chapter 2, pp 16−32.
(12) Hu, Y. S.; Schiraldi, D. A.; Hiltner, A.; Baer, E. *Macromolecules* **2003**, *36*, 3606−3615.
(13) Hu, Y. S.; Liu, R. Y. F.; Schiraldi, D. A.; Hiltner, A.; Baer, E. *Macromolecules* **2004**, *37*, 2136−2143.
(14) Liu, R. Y. F.; Hu, Y. S.; Hibbs, M. R.; Collard, D. M.; Schiraldi, D. A.; Hiltner, A.; Baer, E. *J. Polym. Sci., Part B: Polym. Phys.* **2003**, *41*, 289−307.
(15) Cole, K. C.; Daly, H. B.; Sanschagrin, B.; Nguyen, K. T.; Ajji, A. *Polymer* **1999**, *40*, 3505−3513.
(16) Liu, R. Y. F.; Schiraldi, D. A.; Hiltner, A.; Baer, E. *J. Polym. Sci., Part B: Polym. Phys.* **2002**, *40*, 862−877.
(17) Organ, S. J.; Barham, P. J. *Polym. Prepr.* **1988**, *29*, 602.
(18) Blumstein, R. B. In *Mechanical and Thermophysical Properties of Polymer Liquid Crystals*; Brostow, W., Ed.; Chapman & Hall: London, 1998; Chapter 6, pp 147−171.
(19) Ward, I. M.; Wilding, M. A. *Polymer* **1977**, *18*, 327−335.
(20) Jedlinski, Z.; Franek, J.; Kulczycki, A.; Sirigu, A.; Carfagna, C. *Macromolecules* **1989**, *22*, 1600−1603.
(21) Shilov, S.; Birshtein, T.; Volchek, B. *Makromol. Chem. Theory Simul.* **1993**, *2*, 21−36.
(22) Zubrzycki, I. Z.; Xu, Y.; Madrid, M.; Tang, P. *J. Chem. Phys.* **2000**, *112*, 3437−3441.
(23) Polyakova, A.; Connor, D. M.; Collard, D. M.; Schiraldi, D. A.; Hiltner, A.; Baer, E. *J. Polym. Sci., Part B: Polym. Phys.* **2001**, *39*, 1900−1910.
(24) Liu, R. F. Y.; Hiltner, A.; Baer, E., unpublished results.
(25) Abe, A. *Macromolecules* **1984**, *17*, 2280−2287.
(26) Watanabe, J.; Hayashi, M. *Macromolecules* **1988**, *21*, 278−280.
(27) Hu, Y. S.; Rogunova, M.; Schiraldi, D. A.; Hiltner, A.; Baer, E. *J. Appl. Polym. Sci.* **2002**, *86*, 98−115.
(28) Tokita, M.; Osada, K.; Watanabe, J. *Liq. Cryst.* **1998**, *24*, 477−480.
(29) Watanabe, J.; Hayashi, M. *Macromolecules* **1989**, *22*, 4083−4088.
(30) Benavente, R.; Pereña, J. M.; Pérez, E.; Bello, A. *Polymer* **1993**, *34*, 2344−2347.
(31) Benavente, R.; Pereña, J. M.; Pérez, E.; Bello, A. *Polymer* **1994**, *35*, 3686−3690.
(32) Spies, C.; Zachmann, H. G. *Polymer* **1994**, *35*, 3816−3826.
(33) Chen, D.; Zachmann, H. G. *Polymer* **1991**, *32*, 1612−1621.
(34) Ahumada, O.; Ezquerra, T. A.; Nogales, A.; Baltà-Calleja, F. J.; Zachmann, H. G. *Macromolecules* **1996**, *29*, 5002−5009.
(35) Campo, A. D.; Bello, A.; Pérez, E.; García-Bernabé, A.; Calleja, R. D. *Macromol. Chem. Phys.* **2002**, *203*, 2508−2515.
(36) Wunderlich, B.; Grebowicz, J. *Adv. Polym. Sci.* **1984**, *60/61*, 1−59.
(37) Menczel, J.; Wunderlich, B. *Polymer* **1981**, *22*, 778−782.
(38) Shen, H. C.; McDowell, C. C.; Sankar, S. S.; Freeman, B. D.; Kumpf, R. J.; Wicks, D. A.; Lantman, C. W.; Noël, C. *J. Polym. Sci., Part B: Polym. Phys.* **1996**, *34*, 1347−1361.
(39) Bensaad, S.; Noël, C. *Macromol. Chem. Phys.* **1998**, *199*, 1501−1509.
(40) Diaz-Calleja, R.; Riande, E.; Guzman, J. *J. Polym. Sci., Polym. Phys. Ed.* **1986**, *24*, 337−344.
(41) Diaz-Calleja, R.; Riande, E.; Guzman, J. *Macromolecules* **1989**, *22*, 3654−3659.
(42) Illers, K. H.; Breuer, H. *J. Colloid Sci.* **1963**, *18*, 1−31.
(43) Armeniades, C. D.; Baer, E. *J. Polym. Sci., Part A2* **1971**, *9*, 1345−1369.
(44) Yip, H. K.; Williams, H. L. *J. Appl. Polym. Sci.* **1976**, *20*, 1217−1230.
(45) Hiltner, A.; Baer, E. *J. Macromol. Sci., Phys* **1972**, *B6*, 545−558.
(46) Tonelli, A. E. *J. Polym. Sci., Part B: Polym. Phys.* **2002**, *40*, 1254−1260.
(47) Tsukruk, V. V.; Shilov, V. V.; Lipatov, Y. S. *Acta Polym.* **1985**, *36*, 403−412.
(48) Mazelet, G.; Kléman, M. *J. Mater. Sci.* **1988**, *23*, 3055−3060.
(49) Ford, J. R.; Bassett, D. C.; Mitchell, G. R. *Mol. Cryst. Liq. Cryst.* **1990**, *180B*, 233−243.
(50) Wang, W.; Lieser, G.; Wegner, G. *Macromolecules* **1994**, *27*, 1027−1032.

MA030439M